Narrowband Auscultatory Blood Pressure Measurement

Daniel J. Sebald*, *Member, IEEE*, Dennis E. Bahr, *Senior Member, IEEE*, and Alan R. Kahn, *Life Fellow, IEEE*

***Abstract*—Auscultatory blood pressure measurement uses the presence and absence of acoustic pulses generated by an artery (i.e., Korotkoff sound), detected with a stethoscope or a sensitive microphone, to noninvasively estimate systolic and diastolic pressures. Unfortunately, in high noise situations, such as ambulatory environments or when the patient moves moderately, the current auscultatory blood pressure method is unreliable, if at all possible.**

Empirical evidence suggests that the pulse beneath an artery occlusion travels relatively slow compared with the speed of sound. By placing two microphones along the bicep muscle near the brachial artery under the occlusion cuff, a similar blood pressure pulse appears in the two microphones with a relative time delay. The acoustic noise, on the other hand, appears in both microphones simultaneously.

The contribution of this paper is to utilize this phenomenon by filtering the microphone waveforms to create spatially narrowband information signals. With a narrowband signal, the microphone signal phasing information is adequate for distinguishing between acoustic noise and the blood pressure pulse. By choosing the microphone spacing correctly, subtraction of the two signals will enhance the information signal and cancel the noise signal. The general spacing problem is also presented.

***Index Terms*—Array signal processing, biomedical acoustics, biomedical measurements, biomedical signal processing, blood pressure measurement.**

I. Introduction

AUSCULTATORY blood pressure measurement is the common noninvasive method whereby an air bladder occlusion cuff and pressure gauge (i.e., a sphygmomanometer) is used to fully occlude and then gradually release a patient's brachial artery, and the presence or absence of sound distal to the occlusion near the antecubital fossa is used to identify the pressures at which blood initially begins to flow through the brachial artery (i.e., systolic pressure) and at which normal blood flow returns (i.e., diastolic pressure) [1]. The schematic of Fig. 1 illustrates system elements when the inflated cuff pressure is greater than the instantaneous brachial artery blood pressure. Proximal pressure, p_A, need not be the same as distal pressure, p_B, when the artery is occluded, i.e., $p_A < p_C$ and $p_B < p_C$. Korotkoff [2] first discovered the occurrence of sounds attributed to the pulsatile nature of circulation and

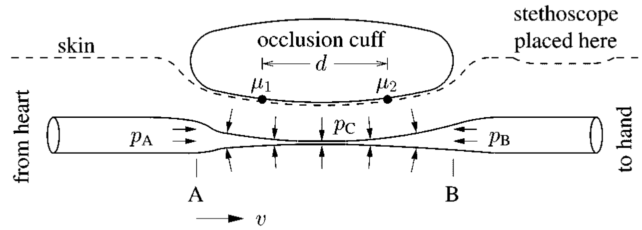

Fig. 1. Schematic of the auscultatory method of blood pressure measurement. Blood flows from left to right.

the presence of an occlusion. For this reason, the resulting auscultatory signal is often referred to as Korotkoff sound. For an example of the Korotkoff sound along with signals from other noninvasive methods used to assess blood pressure see [3].

Power spectra for Korotkoff sound are also given in [3], which show that the auscultatory pulse for a partially or fully occluded brachial artery has most of its energy below 20 Hz. Its spectrum falls off with increasing frequency starting at approximately 25–30 Hz. The frequency content of the Korotkoff sound changes slightly based upon the phase of the blood pressure measuring sequence. For example, the spectrum is broader in phase III—where pulse intensity is a maximum—than in phase IV—where the pulse weakens and becomes muffled. However, an important point is that pulse power spectra for the various Korotkoff phases[1] all share a general fall-off with frequency starting at approximately 25 Hz.

Although auscultatory blood pressure measurement can underestimate systolic pressure by 5–20 mmHg and overestimate diastolic pressure by 12–20 mmHg [4] and there is potential for error due to incorrect cuff sizing [5], the method remains an acceptable standard [6] because of its noninvasiveness and simplicity. There is motivation to automate the Korotkoff method using a microphone and signal processing equipment because of the procedure's ubiquitous nature. Automation is useful for two reasons. First, it allows those unfamiliar with the Korotkoff method to take a blood pressure measurement. Second, it introduces consistency of method thereby eliminating variation due to individual technicians declaring Korotkoff phases differently. The presence of considerable acoustic noise due to microphone sensitivity to patient motion and background noise his limited the success of automation. Therefore, a processing method that rejects acoustic noise is desirable. Furthermore, there are situations where even a trained technician cannot discern the Korotkoff sound from background noise, such as in ambulatory

Manuscript received October 5, 2001; revised March 20, 2002. *Asterisk indicates corresponding author.*

*D. J. Sebald is a freelance engineer. He is at 1553 Adams St. #AB, Madison, WI 53711 USA (e-mail: daniel.sebald@ieee.org).

D. E. Bahr is with Bahr Management, Inc., 3510 West Beltline Hwy, Middleton, WI 53562 USA.

A. R. Kahn is with Human Dimensions, Inc., 1912 Irving Ave. South, Minneapolis, MN 55403 USA.

Publisher Item Identifier 10.1109/TBME.2002.802056.

[1]We use the term "Korotkoff phase" as opposed to the single word "phase" to avoid confusion later with the phasing between multiple microphone signals.

environments. In that case, processing for noise rejection is an enabling technology.

If a pair of microphones, μ_1 and μ_2 in Fig. 1, is positioned under the occlusion cuff in the direction of blood flow (i.e., parallel to the humerus), empirical evidence suggests a pulse wave of the occluded brachial artery takes noticeable time to travel from one microphone to the next, while acoustic noise appears in both microphones simultaneously. Thus, there is potential to process these signals for noise reduction. Although these signals are not the Korotkoff sound, they are closely related. Hence, we retain the name auscultatory. The significant differences between pulses under the cuff and Korotkoff sound is that the pulses under the cuff have a power spectrum in which energy falls off starting at 16 Hz (generally below the audible range) and there is no muffling of the signal as there is in the case of phase IV Korotkoff sound.

The pair of occlusion cuff microphones can be viewed as the simplest instance of a linear sensor array. Therefore, we aim to utilize signal processing principles which have been shown to be advantageous in other array processing scenarios [7], [8]. The approach here is to bandpass filter the microphone signals to create a spatially narrowband pulse information signal and to choose the microphone spacing such that the information signal exhibits an 180° phase difference between the two microphones. The choice of 180° phasing is meant to simplify processing.

The paper continues as follows. Section II presents new innovations for processing the auscultatory microphone signals, including the concept of narrowband signals. Section III gives some examples of noisy auscultatory signals and the resulting processed waveforms. Section IV discusses several characteristics of the narrowband method observed by the authors. Included is a discussion of ancillary topics such as signal processing for pulse detection and limitations to determining Korotkoff phase. Also, an example of Korotkoff cycle pulse data is given. The Appendix contains a description of the general system when microphone spacing cannot be selected to create the all real signal system of Section II.

II. Auscultatory Signal Processing

The main signal processing technique for extracting the blood pressure signal from noise is to exploit the fact that the pressure pulse wavefront under the occlusion cuff moves along the arm at a slow rate compared with acoustic noise appearing in the microphone pair. The sensor signals are represented by functions $\mu_i(t) : \mathbb{R} \mapsto \mathbb{R}$, $i = 1, 2$, where t is time. Let $m(t) : \mathbb{R} \mapsto \mathbb{R}$ be the pulse information bearing signal, and let $\eta(t) : \mathbb{R} \mapsto \mathbb{R}$ be the acoustic noise signal common to both sensors. For simplicity of exposition, we leave any uncorrelated noise between sensors out of the model. If $\mu_1(t)$ is the reference sensor signal where the second sensor is positioned further from the heart, then

$$\mu_i(t) = m\left(t - \frac{(i-1)d}{v}\right) + \eta(t)$$

where v is waveform velocity and d is sensor spacing. In general, processing to extract $m(t)$ is difficult. However, when the various signals at play are spatially *narrowband*, some alternatives for signal processing exist.

For a signal $x_i(t) : \mathbb{R} \mapsto \mathbb{R}$ to be narrowband technically means that its modulation coherence distance exceeds the array width [7], [9], which in this two microphone scenario is the spacing d. Since in our model, noise is assumed coherent, $\eta(t)$ has an infinite coherence distance and therefore is always spatially narrowband even though temporally it may occupy a wide frequency range. On the other hand, for the information signal, the narrowband property implies two things. First, the information signal is sinusoidal in nature, i.e.,

$$x_i(t) = m'\left(t - \frac{(i-1)d}{v}\right) \times \cos\left(2\pi f\left(t - \frac{(i-1)d}{v}\right) + \psi\right) + \eta'(t)$$

where f is temporal frequency in Hz and ψ is a phase factor in radians. The prime of $m'(t)$ simply means that the information signal is derived from $m(t)$ in a fashion that $m'(t)$ is still useful for the purpose of determining blood pressure. Similarly, $\eta(t)$ may be altered to $\eta'(t)$ in the process. The second implication of being narrowband is that $m'(t-(i-1)d/v) \approx m'(t)$. Thus

$$x_i(t) \approx m'(t)\cos\left(2\pi f t - \frac{f(i-1)d}{v} + \psi\right) + \eta'(t) \qquad (1)$$

and if we choose the spacing d given frequency f and velocity v so that a 180° phase difference for the sinusoid exists between the two microphones, we have

$$\begin{aligned} x_1(t) &= m'(t)\cos(2\pi f t + \psi) + \eta'(t) \\ x_2(t) &\approx -m'(t)\cos(2\pi f t + \psi) + \eta'(t). \end{aligned}$$

It is now evident that the strategy is to simply subtract one half $x_2(t)$ from one half $x_1(t)$ to remove the noise signal and recover the information signal, i.e.,

$$\frac{1}{2}x_1(t) - \frac{1}{2}x_2(t) \approx m'(t)\cos(2\pi f t + \psi). \qquad (2)$$

Alternate methods of processing the narrowband signals are possible, e.g., see [10]. However, the subtraction method has the advantage of being a linear process, and it is directly related to array processing [7], [11], [12], thus providing a sound theoretical basis.

We now describe how to make the two auscultatory microphone signals narrowband. Fig. 2 shows a block diagram of the various analog and discrete-time processing components of the blood pressure measurement system. Let $\tilde{\mu}_1(t)$ and $\tilde{\mu}_2(t)$ be the analog microphone signals. (The tilde means unbalanced.) These signals are what have been used for processing in systems such as [13] and are generally not narrowband signals. The most important processing step, first proposed in [14], is to apply a 15–50 Hz bandpass analog filter. The reasons are twofold. First, this removes the high-power, low-frequency noise from the system that would otherwise saturate analog-to-digital (A/D) converters. Second, the blood pressure pulses become narrowband. Recall that the natural power spectrum of the blood pressure pulses falls off with frequency starting at approximately 16 Hz. Applying a filter with frequency response falling off toward 0 Hz starting at 15 Hz, gives the pulses a narrowband appearance.

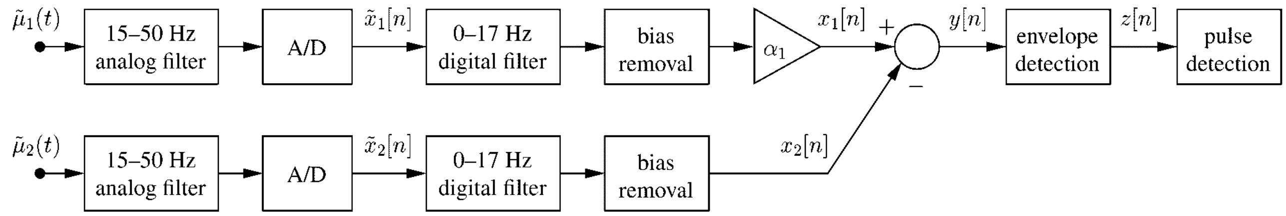

Fig. 2. Elements of a narrowband auscultatory blood pressure measurement system when microphone spacing is chosen to be half the wavelength. The scaling factor of one half in (2) is disregarded because pulse detection algorithms are amplitude independent or can be adjusted accordingly.

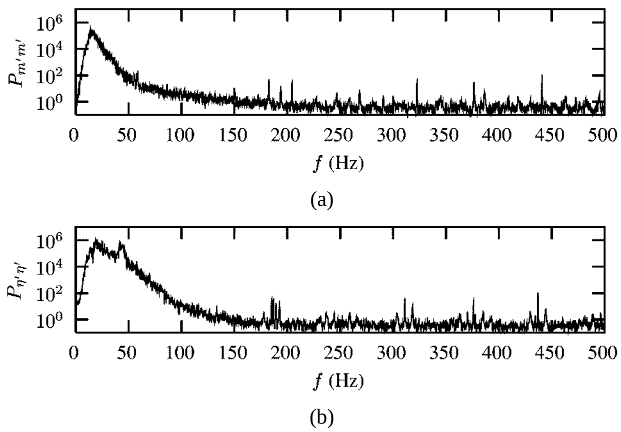

Fig. 3. Power spectral density of the bandpass filtered (a) cuff auscultatory waveform free of noise and (b) ambulance noise without auscultatory signal.

Fig. 3 shows the power spectra for bandpass filtered auscultatory signals under the occlusion cuff for pressure pulses and ambulance noise, individually. The filtered blood pressure signal has the spectrum of a modulated sinusoid, whereas the noise has a broader spectrum. Blood pressure pulses near diastolic do deviate slightly from the narrowband model. Also, for lower grade microphone units, cuff noise can exhibit coupling and other noncoherent effects. Therefore, further filtering is beneficial in some scenarios. As illustrated in Fig. 2, after A/D conversion is a low-pass digital filter with cutoff just above the center frequency of the narrowband blood pressure pulses. This forces all signals to have a narrow temporal frequency range to ensure suitability with the array processing model. However, the analog filter cuton and digital filter cutoff should be set far enough away from the center frequency so that moderately high heart rate pulses are not attenuated.

After the low-pass filter is the balancing stage. This consists of removing any biases introduced by the A/D converters. Such biases tend to confuse balancing algorithms. Then an adaptive algorithm (not illustrated in Fig. 2) computes the gain from one channel to the other channel, α_1. The appropriate channel is then multiplied by this gain, after which one signal is subtracted from the other.[2] The resulting signal is then used for pulse detection.

A variety of algorithms exist for computing the gain α_1, and this processing step requires great attention. Squaring the signals or taking their absolute value is the first element of computing the gain. Following this with a single-tap, sample-adaptive algorithm, such as the least-mean-squared (LMS) algorithm or its variants [15], is convenient. The disadvantage of the LMS algorithm is that its adaptation rate is based upon the power of its input. Thus, depending upon how the LMS update constant is selected, the gain computation tends to stick at one point if its input channel is one of low power, or it tends to adapt too quickly if its input channel is one with significant power. The sign–sign variation of the LMS algorithm eliminates this problem since upon every iteration it adjusts a set amount in a positive or negative direction. Also, as a practical matter, an adaptive algorithm does not converge properly when its input or desired signal saturates. Thus inherent in computing α_1 is a mechanism for detecting saturation and turning off adaptation in such situations.

The final stage of processing, that of extracting the information signal $m'(t)$, also presents a variety of alternatives, many of which are well studied for applications having narrowband signals, such as pulsed radar [16]. Methods are generally of the form of squaring the signal or taking its absolute value then low-pass filtering. These simple envelope detection methods work because only the intensity of the pulses is of interest. From our viewpoint, $m'(t)$ is a positive signal, and the phase ψ remains constant during each pulse but may change from pulse to pulse.

We conclude this section by discussing the microphone spacing d and the gain characteristics as a function of pulse velocity v. As mentioned earlier, when the distance between the microphones is chosen correctly, the two 16-Hz narrowband auscultatory signals will be approximately 180° out of phase. This distance was found empirically to be approximately 2.5 cm, and it corresponds to half the wavelength, λ, of the filtered traveling auscultatory wave of center frequency f. Hence, the traveling wave speed under the cuff is roughly

$$v = \lambda f = 2\,d\,f = 2 \times 2.5 \text{ cm} \times 16 \text{ Hz} = 80 \text{ cm/s}.$$

This propagation rate agrees with that observed in [13] and is discussed later.

To get some idea of how sensitive the difference $y(t)$ is to the traveling wave speed v, we consider the gain of the microphone system. Because of the narrowband nature of input signals, the subtraction process can be viewed as a modulated sinusoid passed through a linear system with impulse response $(1/2)\delta(t) - (1/2)\delta(t - (d/v))$. As such, the gain for the system is simply the magnitude of the Fourier transform of the linear system [17]. That is

$$g_{2.5}(v) = \frac{1}{2}\left|1 - e^{j2\pi(16)(2.5)/v}\right|$$

[2]A good practice is to keep track of gains in both directions for the channels and utilize whichever gain is larger. This avoids the situation of significantly attenuating channel one when channel two is a weak signal.

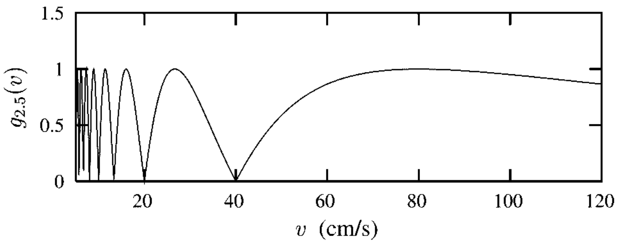

Fig. 4. Gain for the narrowband system as a function of linear flow velocity when microphone spacing is 2.5 cm.

where $g_{2.5}(v)$ is the gain for the difference when microphone spacing is 2.5 cm. The gain is shown in Fig. 4 as a function of velocity. For a velocity of 80 cm/s the gain is one, and as the velocity approaches ∞ (the effective noise velocity) the gain tends toward zero. The appealing result is that performance is not severely sensitive to propagation velocity. A blood pressure pulse traveling under the occlusion cuff in the range of 60 to 120 cm/s may be processed reasonably well.

III. Example

Fig. 5 shows processing results for blood pressure signals plus ambulance noise signals. The top two traces are signals $\tilde{x}_1[n]$ and $\tilde{x}_2[n]$, respectively, somewhere in the middle of an auscultatory blood pressure measurement cycle (i.e., Korotkoff cycle). The signal-to-noise ratio (SNR) is low enough in these two waveforms that the auscultatory signal is unrecognizable when considering each signal individually. The third signal is the difference signal $y[n]$ of the two top traces after low-pass filtering and balancing, and it shows significant improvement in SNR. The balancing algorithm was a sign–sign, sample update adaptive filter with a single tap which converged to approximately 2.0 for α_1. The bottom trace in Fig. 5 is the extracted envelope $z[n]$ computed from $y[n]$ by taking its absolute value and low-pass filtering.

IV. Discussion

When occlusion cuff pressure is above diastolic pressure, the arteries beneath the cuff are constricted between beats. The vessels are continuously constricted when cuff pressure is above systolic pressure. When cuff pressure is between diastolic and systolic, blood enters the constricted segment due to the traveling pressure pulse originating from the heart. The large compliance the artery exhibits when exposed to the pressure wavefront results in a slowed pulse wave through the cuff arterial segment. This is the phenomenon detected by the proposed system. One observation is that this phenomenon is not significantly effected by the arterial tree distal to the cuff. For example, in the case of low perfusion to the forearm and hand, the slowed pulse beneath the cuff can still be detected. However, the Korotkoff sound of the traditional method is often difficult to detect in such a scenario.

An accurate computation for the velocity of the slowed pressure wave beneath the cuff is difficult because of the arched shape of the occlusion and the fact that the wave is distorted by the occlusion. The velocity of 80 cm/s, computed from phasing information of a narrowband signal, is likely not consistent along the occlusion, but the distributed velocity is not of great importance. The proposed method only observes two points spatially and utilizes a narrow frequency band. We have observed rather consistent velocity among test subjects.

The velocity of the pressure wave when there is no occlusion is approximately 800 cm/s for the brachial artery, which is about 40 cm from the aorta arch [18]. The gain for $y[n]$ is 0.16 at 800 cm/s. This suggests that the pulse signal detected when the brachial artery is not occluded will be sufficiently rejected when processed to generate $y[n]$.

Korotkoff phase cannot be determined for individual pulses using the proposed technique. This is true for two reasons. First, the point of observation under the cuff will not exhibit turbulence as occurs near the antecubital fossa. The muffling sound of turbulence is often used to identify the final Korotkoff phase. Second, and more important, the process of creating narrowband signals loses all information about spectral content which is required in methods such as [19]. More will be said on this matter shortly.

There still remains the issue of pulse detection as a secondary step in an automated Korotkoff cycle. The narrowband pulses generated by spatial processing have the characteristics of a radio-frequency (RF) pulse. As such, the spatially processed waveform can be further processed with conventional RF methods, as discussed in [16]. For example, pulses can be declared based upon dynamic level crossings and the position and amplitude of the pulses can be chosen where the output $z[n]$ is maximum. Furthermore, after determining the pulse locations and intensities, statistics can be used to remove false alarms and reconstruct misses. Fig. 6 is an example Korotkoff pulse cycle attained with such methods when the microphone pair is positioned between the bicep and tricep of the inner arm. The occlusion cuff was tapped to the extent of creating considerable noise on the level of that shown in Fig. 5. Along the y-axis of Fig. 6 is unit-less pulse intensity. The striking property of the sequence is the quick transition in intensity that occurs near systolic and diastolic pressures, just as with the onset and abatement of Korotkoff sound. The particular cycle of Fig. 6 shows a local valley just after, what is believed to be, systolic pressure and shortly before, what is believed to be, diastolic pressure. This was commonly observed in recordings among test subjects, but is not always present. The reason for this is not known. This phenomenon requires further study, but some issues to investigate are emptying of the distal portion of the artery before the first occlusion opening, influence of microphone casing on arterial compression, or an unaccounted for artifact of the array processing method.

As alluded to previously, since Korotkoff phase information is lost using the narrowband technique, a consistent method for establishing the beginning and end of a Korotkoff cycle, i.e., estimating systolic and diastolic pressures, must be applied to the Korotkoff cycle pulse intensity data. For example, one could declare the beginning (end) of a cycle to be just before (after) the amplitude of pressure pulses rises (falls) to 50% (30%) of the average of four maximum pulse intensities in the mid cycle region. Fig. 6 shows with a cross the pulses chosen for systolic and diastolic pressures using this simple method. The resulting blood pressure by this estimation is 139/93 mmHg.

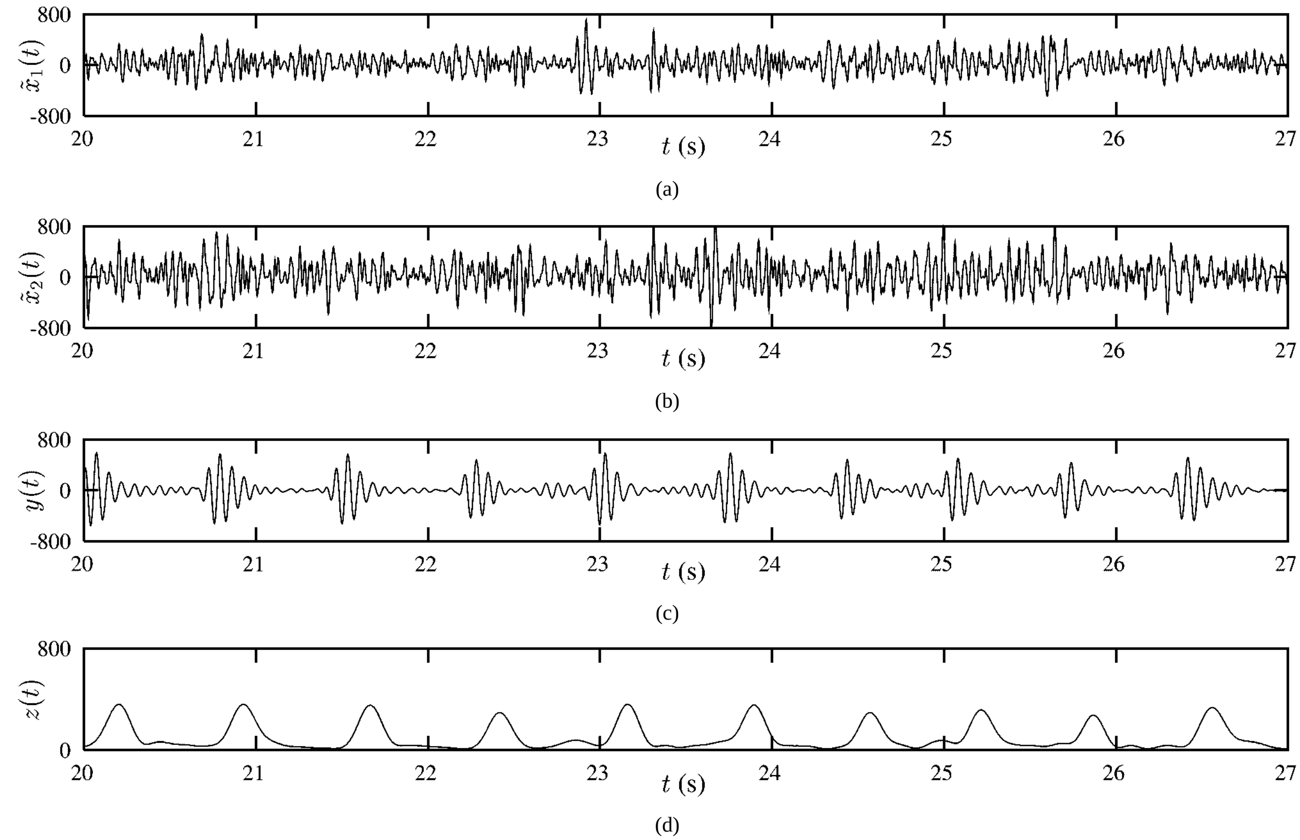

Fig. 5. Various signals of the narrowband auscultatory blood pressure measurement system. (a) and (b) The two microphone inputs of filtered auscultatory pulse signals summed with filtered ambulance noise signals. (c) The narrowband filtered difference signal, clearly reducing noise to reveal sinusoidal pulses. (d) The extracted envelope derived by low-pass filtering the absolute value of the difference signal.

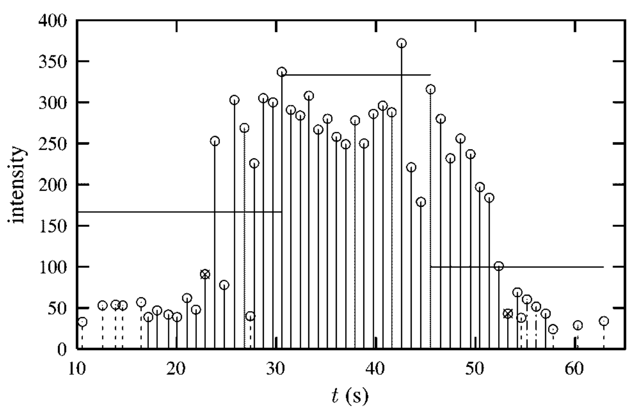

Fig. 6. Pulses detected for a Korotkoff cycle using the narrowband auscultatory method. As determined by secondary processing, pulses with dot stems are false alarms and pulses with dash/dot stems are misses. The top horizontal line is the computed plateau. The bottom horizontal lines are 50% and 30% of the plateau for systolic and diastolic, respectively. The pulses marked with crosses are the declared systolic and diastolic pulses.

V. Conclusion

Narrowband array processing of the pressure waveform generated under an occlusion cuff near the brachial artery can be used to estimate systolic and diastolic blood pressures. Although the detected signals do not have frequency content in the audible range, the name auscultatory has been used to describe the method because microphones are used in a fashion similar to the traditional method, and the characteristics of the processed pulse data bear a resemblance to Korotkoff sound behavior. An example for data acquired in an ambulance shows the significant processing gain that can be achieved in noisy environments with this new method.

Empirical results suggest occluded pulse pressure wave velocity is somewhere around 80 cm/s. With system parameters chosen to provide a gain of one for narrowband signals with this velocity, plots of array gain show that the system has a wave velocity range of approximately 60–120 cm/s. This should provide reasonable robustness to random deviation of pulse velocity among patients.

The proposed method cannot determine the Korotkoff phase of a pulse based upon frequency content. Therefore, it remains to be seen how well derived pulse data correlates with blood pressure readings from traditional auscultatory methods. However, we believe accurate blood pressure readings can be made from the narrowband auscultatory technique because of the clear transition regions observed for pulse intensity data in a Korotkoff cycle. A precise and accurate blood pressure estimation algorithm using narrowband auscultatory Korotkoff cycle data requires further research. In some tests, the pulse intensity Korotkoff cycle data exhibits local peaks at the systolic and diastolic transition regions. This phenomenon has not been explained.

Related to accuracy is the issue of optimal microphone placement. Our initial findings are that the narrowband auscultatory method does not require that microphones be placed directly over an artery. In fact, in some cases, microphone placement

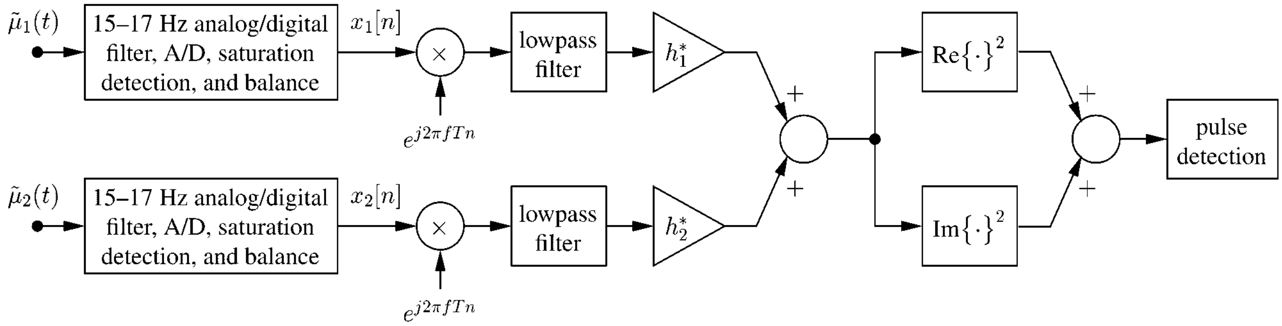

Fig. 7. Elements of a narrowband auscultatory blood pressure measurement system for general microphone spacing, where T is the sample period.

under the cuff and above a muscle mass near the artery appears to produce a good result. Again, further research on this issue is required.

APPENDIX

In some applications it may be the case that a microphone spacing d of 2.5 cm is too large. If we want to reduce d and it is not possible to proportionally adjust the center frequency f of the blood pressure information signal, we are left to process signals using orthogonal components, i.e., sines and cosines. This approach may be represented more compactly using complex notation. Consider that (1) can be expressed as

$$x_i(t) \approx \mathrm{Re}\left\{\left[m'(t)e^{-j2\pi f(i-1)d/v} + \eta'_{\mathbb{C}}(t)\right] e^{j(2\pi ft+\psi)}\right\} \quad (3)$$

where $\eta'_{\mathbb{C}}(t) : \mathbb{R} \mapsto \mathbb{C}$ is the complex *baseband* representation of the altered noise. Equation (3) is the general notation commonly used in array processing where spatial filters generally have complex coefficients.

For convenience, define phasing vector

$$\mathbf{s}(d) = [\,1 \quad e^{-j2\pi fd/v}\,]^T$$

where ^{T} is vector transpose, so that when the sensor signals are put in vector form

$$\begin{aligned}\mathbf{x}(t) &= [\,x_1(t) \quad x_2(t)\,]^T \\ &= \mathrm{Re}\left\{[m'(t)\mathbf{s}(d) + \eta'_{\mathbb{C}}(t)\mathbf{s}(0)]\, e^{j(2\pi ft+\psi)}\right\}.\end{aligned}$$

To process, the complex baseband signals must first be extracted from the measured real signals. Multiplying the real signals by a complex sinusoid of frequency f yields

$$\mathbf{x}(t)e^{j2\pi ft} = \frac{1}{2}\Big([m'(t)\mathbf{s}(d) + \eta'_{\mathbb{C}}(t)\mathbf{s}(0)]\, e^{j(4\pi ft+\psi)} + [m'(t)\mathbf{s}(d) + \eta'_{\mathbb{C}}(t)\mathbf{s}(0)]^*\, e^{-j\psi}\Big) \quad (4)$$

where * is complex conjugate. The first term of the right-hand side of (4) may be removed using a low-pass temporal filter. The second term of the right-hand side of (4) is then multiplied by a spatial filter

$$\mathbf{h} = [\,h_1 \quad h_2\,]^T$$

to isolate the information signal and reject the noise component. A phase factor of ψ remains for the second term, but this can be easily removed with a square-law type detector. With such a detector, the fact we are processing the complex conjugate of the information signal is irrelevant.

Fig. 7 illustrates the general method of array processing for auscultatory signals. After modulation of the narrowband signals follows the low-pass filters. This amounts to four filters (two per complex waveform), whereas the real system of Fig. 2 requires a single low-pass filter in the envelope detection stage. After the low-pass filters is the spatial filter with complex-valued coefficients. Following the spatial filter is the square law detector. Since this computes the square of the information envelope, allowing for some noise, no envelope detector is required in the pulse detector of Fig. 7.

The spatial filter coefficients must be chosen so that the information signal has a gain of one and the noise has a gain of zero, i.e.,

$$\begin{aligned}\mathbf{h}^H\mathbf{s}(d) &= 1,\\ \mathbf{h}^H\mathbf{s}(0) &= 0\end{aligned}$$

where ^{H} is complex conjugate vector transpose, which means

$$\mathbf{h} = \begin{bmatrix}\mathbf{s}^H(d)\\ \mathbf{s}^H(0)\end{bmatrix}^{-1}\begin{bmatrix}1\\0\end{bmatrix} \quad (5)$$

provided the phasing matrix is nonsingular. The gain for the more general system follows from an argument similar to that at the end of Section II and is

$$g_d(v) = \left|h_1^* + h_2^*\, e^{j2\pi fd/v}\right|.$$

As an example, with a spacing of one quarter wavelength, i.e., $d = 1.25$ cm, the filter coefficients become

$$\begin{aligned}\mathbf{h} &= \begin{bmatrix}1 & j\\ 1 & 1\end{bmatrix}^{-1}\begin{bmatrix}1\\0\end{bmatrix}\\ &= \frac{1}{2}\begin{bmatrix}1+j\\ -1-j\end{bmatrix}.\end{aligned}$$

(Also, note that when $d = 2.5$ cm in (5), the filter coefficients equal that of the half-wavelength narrowband system in (2), as should be the case.) As a comparison with the half-wavelength narrowband system, the gain for the quarter-wavelength system

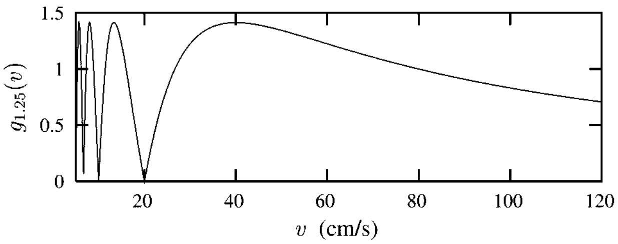

Fig. 8. Gain for the narrowband system as a function of linear flow velocity when microphone spacing is 1.25 cm.

is shown in Fig. 8. As designed, the system gain is one for a narrowband pulse traveling at 80 cm/s. However, the response exhibits a gain of $\sqrt{2}$ off 80 cm/s, whereas the maximum gain for the system of Fig. 2 is one. All things considered, the usable range for the velocity is approximately the same for the half-wavelength and quarter-wavelength systems, 60–120 cm/s.

Acknowledgment

The authors thank the reviewers for their thoughtful comments and suggested changes, which have improved this paper.

References

[1] G. M. Drzewiecki, "Modeling of noninvasive arterial blood pressure methods," in *Analysis and Assessment of Cardiovascular Function*, G. Drzewiecki and J. K.-J. Li, Eds. New York: Springer-Verlag, 1998, ch. 13, pp. 203–221.

[2] N. C. Korotkoff, "On the subject of methds of determining blood pressure," *Bull. Imperial Mil. Med. Acad. St. Petersburg*, vol. 11, pp. 365–367, 1905.

[3] G. Drzewiecki, J. Melbin, and A. Noordergraaf, "Noninvasive blood pressure recording and the genesis of Korotkoff sound," in *Handbook of Bioengineering*, R. Skalak and S. Chien, Eds. New York: McGraw-Hill, 1987, ch. 8, pp. 8.1–8.36.

[4] S. B. London and R. E. London, "Comparison of indirect blood pressure measurements (Korotkoff) with simultaneous direct brachial artery pressure distal to cuff," *Adv. Intern. Med.*, vol. 13, pp. 127–142, 1967.

[5] L. A. Geddes and S. J. Whistler, "The error in indirect blood pressure measurement with incorrect size of cuff," *Amer. Heart J.*, vol. 96, pp. 4–8, 1978.

[6] W. B. White, A. S. Berson, C. Robbins, M. J. Jamienson, L. M. Prisant, E. Roccella, and S. G. Sheps, "National standard for measurement of resting and ambulatory blood pressures with automated sphygmomanometers," *Hypertension*, vol. 21, no. 4, pp. 504–509, Apr. 1993.

[7] J. E. Hudson, *Adaptive Array Principles*. New York: Inst. Elect. Eng/Peregrinus, 1981.

[8] S. Haykin, Ed., *Array Signal Processing*. Englewood Cliffs, NJ: Prentice-Hall, 1985.

[9] B. Van Veen, "Minimum variance beamforming," in *Adaptive Radar Detection and Estimation*, S. Haykin and A. Steinhardt, Eds. New York: Wiley, 1992, ch. 4, pp. 161–236.

[10] A. R. Kahn, D. E. Bahr, and K. W. Allen, "Blood pressure monitoring with improved noise rejection," 5 873 836, Feb. 1999.

[11] S. Haykin, *Adaptive Filter Theory*. Englewood Cliffs, NJ: Prentice-Hall, 1991.

[12] D. J. Sebald and B. D. Van Veen, "Application of MVDR beamforming to reject turbulence noise in a duct," in *Proc. IEEE Int. Conf. Acoust., Speech, Signal Processing*, Atlanta, GA, May 1996, pp. 2734–2737.

[13] P. R. Voith, "Blood pressure measuring method and apparatus," 5 649 535, July 1997.

[14] A. R. Kahn, D. E. Bahr, and K. W. Allen, "Method and apparatus for detecting blood pressure by blood pressure sounds in the presence of significant noise," 5 680 868, Oct. 1997.

[15] J. A. Bucklew, T. G. Kurtz, and W. A. Sethares, "Weak convergence and local stability properties of fixed step size recursive algorithms," *IEEE Trans. Inform. Theory*, vol. 30, pp. 966–978, May 1993.

[16] H. R. Raemer, *Statistical Communication Theory and Applications*. Englewood Cliffs, NJ: Prentice-Hall, 1969.

[17] A. Budak, *Circuit Theory Fundamentals and Applications*. Englewood Cliffs, NJ: Prentice-Hall, 1978.

[18] W. W. Nichols and M. F. O'Rourke, *McDonald's Blood Flow in Arteries: Theoretical, Experimental and Clinical Principles*, 4 ed. Arnold, London, U.K., 1998.

[19] A. Maurer and A. Noordergraaf, "Korotkoff sound filtering for automated three-phase measurement of blood pressure," *Amer. Heart J.*, vol. 91, pp. 584–591, 1976.

Daniel J. Sebald (S'89–M'01) received the B.S. degree from the Milwaukee School of Engineering, Milwaukee, WI, in 1987, the M.S. degree from Marquette University, Milwaukee, in 1992 and the Ph.D. degree from the University of Wisconsin, Madison, in 2000, all in electrical engineering.

He is a registered P.E. in the state of Wisconsin and has worked for Camtronics Medical Systems, Hartland WI, Nicolet Instrument Technologies, Madison, Xyte, Madison, and OB Scientific, Germantown WI. His research interests include signal processing, communications, real-time DSP and medical technology.

Dennis E. Bahr (S'65–M'68–SM'75) was born in Wausau, WI, in 1943. He received the B.S.E.E. and M.S.E.E. degrees from the University of Wisconsin, Madison, in 1968 and 1972, respectively.

He was an Adjunct Professor in the Department of Electrical and Computer Engineering at the University of Wisconsin, Madison (1980–1990) where he taught courses in logic design and advanced digital design. He owns and operates his own consulting business where he is involved in the management, research, and development of products for the biomedical instrumentation and medical fields. He participated in a team that developed the first practical intracranial pressure monitor and managed a team that developed a vital signs monitor and a pulse oximeter that have been very successful in the hospital market place. His current projects include a fetal oximeter and a blood pressure system that will operate in severe motion.

Mr. Bahr is a member of Sigma Xi, the scientific research society, and an Associate Fellow of the AIAA. He is a Registered Professional Engineer in the State of Wisconsin. He has written 21 papers, a chapter in *Essential Noninvasive Monitoring in Anesthesia* (New York: Grune & Stratton, 1980), and holds 11 U.S. patents.

Alan R. Kahn (F'73–LF'97) received the M.D. degree from the University of Illinois, Chicago, in 1959.

He invented and developed numerous clinical biomedical products. He was a founder and President of the Alliance for Engineering in Medicine and Biology, Founding Member of the American Institute of Biological and Medical Engineering, and has held top technical management positions in biomedical companies including Medtronic, Beckman Instruments, and Hoffman-La Roche. His academic activities included professorial appointments in Electrical and Computer Engineering at the University of Cincinnati, in Anesthesiology at the University of Illinois, in Neurosurgery at the University of Wisconsin, and in Laboratory Medicine and Pathology at the University of Minnesota.

Dr. Kahn holds 18 patents and has participated in the invention and development of six blood pressure monitoring products, one of which was the first to measure the blood pressure of astronauts and pilots flying high-performance aircraft.